Food Research International 165 (2023) 112519

Contents lists available at ScienceDirect

Food Research International

journal homepage: www.elsevier.com/locate/foodres

Curcumin and 10-undecenoic acid as natural quorum sensing inhibitors of LuxS/AI-2 of *Bacillus subtilis* and LasI/LasR of *Pseudomonas aeruginosa*

Susana Fernandes [a,b], Anabela Borges [a,b], Inês B. Gomes [a,b], Sérgio F. Sousa [c], Manuel Simões [a,b,*]

[a] *LEPABE - Laboratory for Process Engineering, Environment, Biotechnology and Energy, Faculty of Engineering, University of Porto, Rua Dr. Roberto Frias, 4200-465 Porto, Portugal*
[b] *ALiCE - Associate Laboratory in Chemical Engineering, Faculty of Engineering, University of Porto, Rua Dr. Roberto Frias, 4200-465 Porto, Portugal*
[c] *UCIBIO/REQUIMTE, BioSIM, Departamento de Biomedicina, Faculdade de Medicina da Universidade do Porto, Alameda Prof. Hernâni Monteiro, 4200-319 Porto, Portugal*

ARTICLE INFO

Keywords:
Molecular docking
Phytochemicals
Quorum sensing inhibition
Virtual screening

ABSTRACT

The quorum sensing (QS) system is related to cell-to-cell communication as a function of population density, which regulates several physiological functions including biofilm formation and virulence gene expression. QS inhibitors have emerged as a promising strategy to tackle virulence and biofilm development. Among a wide variety of phytochemicals, many of them have been described as QS inhibitors. Driven by their promising clues, this study aimed to identify active phytochemicals against LuxS/autoinducer-2 (AI-2) (as the universal QS system) from *Bacillus subtilis* and LasI/LasR (as a specific QS system) of *Pseudomonas aeruginosa*, through *in silico* analysis followed by *in vitro* validation. The optimized virtual screening protocols were applied to screen a phytochemical database containing 3479 drug-like compounds. The most promising phytochemicals were curcumin, pioglitazone hydrochloride, and 10-undecenoic acid. *In vitro* analysis corroborated the QS inhibitory activity of curcumin and 10-undecenoic acid, however, pioglitazone hydrochloride showed no relevant effect. Inhibitory effects on LuxS/AI-2 QS system triggered reduction of 33–77% by curcumin (at 1.25–5 μg/mL) and 36–64% by 10-undecenoic acid (at 12.5–50 μg/mL). Inhibition of LasI/LasR QS system was 21% by curcumin (at 200 μg/mL) and 10–54% by 10-undecenoic acid (at 15.625–250 μg/mL). In conclusion, *in silico* analysis allowed the identification of curcumin and, for the first time, 10-undecenoic acid (showing low cost, high availability, and low toxicity) as alternatives to counteract bacterial pathogenicity and virulence, avoiding the imposition of selective pressure usually related to classic industrial disinfection and antibiotics therapy.

1. Introduction

Quorum sensing (QS) is a cell-to-cell signalling process used to regulate gene expression as a function of population density. The QS mechanism involves the production and release of small chemical molecules, known as autoinducers (AIs), and cell response to the level of AIs (Hawver et al., 2016). Above a minimum threshold level, AIs are recognized by specific receptors in the cytoplasm or cell membrane. The activated receptors start a signal transduction cascade or repression of target genes, resulting in population-wide changes in the phenotype (Atkinson & Williams, 2009). Among regulated physiological functions, QS regulates virulence gene expression (*i.e.* exoprotease, elastase, phospholipase, lectin, surfactin, sporulation), motility, symbiosis, and biofilm formation, increasing cell resistance to antimicrobial agents and host pathogenicity (Brindhadevi et al., 2020). Based on the differences among AI molecules, QS is classified into four types. Two of them are LuxI/LuxR and autoinducing peptide (AIP) QS systems. Both are species-specific and used for intraspecies communication in Gram-negative and -positive bacteria, respectively. Other QS systems are LuxS/AI-2 QS system for interspecies communication and the AI-3 epinephrine/norepinephrine QS system used for signalling between bacteria and their hosts (Zhang et al., 2019).

This study focused on the species-specific LasI/LasR QS system of *Pseudomonas aeruginosa*, the most studied QS mechanism (Whitehead et al., 2001), and on the universal LuxS/AI-2 QS system operating in *Bacillus subtilis* (Duanis-Assaf et al., 2015). LasI/LasR QS system is

* Corresponding author at: LEPABE - Laboratory for Process Engineering, Environment, Biotechnology and Energy, Faculty of Engineering, University of Porto, Rua Dr. Roberto Frias, 4200-465 Porto, Portugal.
E-mail address: mvs@fe.up.pt (M. Simões).

https://doi.org/10.1016/j.foodres.2023.112519
Received 24 October 2022; Received in revised form 6 January 2023; Accepted 21 January 2023
Available online 24 January 2023

activated by *N*-(3-oxododecanoyl)-L-homoserine lactone (3-oxo-C12-HSL) (Bottomley et al., 2007). LasI catalysis the formation of 3-oxo-C12-HSL from a fatty acyl-acyl carrier protein (acyl-ACP) and S-adenosyl-L-methionine (SAM), while LasR is activated by 3-oxo-C12-HSL, which triggers virulence expression (Bottomley et al., 2007). In LuxS/AI-2 QS system, LuxS catalysis the cleavage of S-ribosylhomocysteine (RHC) to homocysteine and 4,5-dihydroxy-2,3-pentadione that spontaneously cyclizes to form AI-2 (Schauder et al. 2001). LuxP/Q recognizes AI-2, resulting in the inactivation of LuxO and production of LuxR that is responsible for the transcription of virulence genes (Ng and Bassler, 2009).

In food industrial settings, biofilm formation is responsible for several technical and economic problems, and also the accumulation of unwanted and spoilage microorganisms (Bozzoli et al., 2020; Petit et al., 2013). Thus, to ensure high operating productivity and high safety conditions, production lines are often cleaned daily using antimicrobial treatments (Li et al., 2019). However, the biofilm lifestyle allows microbial survival to antimicrobials even in the presence of critical exposure concentrations (Fernandes et al., 2022). This concern has led to the search for alternative and more efficient antimicrobial strategies. A potential strategy involves the application of QS inhibitors in combination with current antimicrobial agents. The upregulation of QS during antimicrobial treatment is related to the inefficacy of the approaches used for sessile microbial control (Li et al., 2022). Additionally, several authors have demonstrated that the attenuation of the expression of virulence factors and the prevention of biofilm formation can occur by interfering with the QS system (Borges et al., 2017; Kim et al., 2015; Mayer et al., 2020; Wei et al., 2020). Thus, QS inhibition not only leads to the mitigation of pathogenesis and microbial virulence but also potentiates microbial susceptibility to antimicrobial agents.

There are several phytochemicals (compounds from the secondary metabolism of plants) that have already been identified as QS inhibitors (Bali et al., 2019; Chakraborty et al., 2020; Zhong et al., 2020). However, there is a lack of scientific knowledge about their safety and possible toxic effects, which hinders their application (Hintz et al., 2015). The search for phytochemicals with anti-QS activity and chemical and environmental safety aiming for a translational application is an ongoing process. This study aims to select new active phytochemicals (with recognized low toxicity) against LuxS/AI-2 QS of *B. subtilis* and LasI/LasR QS of *P. aeruginosa* using *in silico* analysis. The target for QS inhibition studies can be proteins involved in the production (*i.e.* LasI and LuxS) or recognition/detection of AIs (*i.e.* LasR). An *in silico* approach allows the selection of phytochemicals with potential anti-QS activity from a large database, which should be *in vitro* validated (Puertas-Martin et al., 2020). For that, molecular docking and virtual screening were optimized and applied to screen thousands of phytochemicals (only drug-like compounds) and pick the most prospective ones to be used for *in vitro* validated using reporter strains *Vibrio harveyi* BB170 and *P. aeruginosa* PA14-*R*3, responsive to AI-2 and 3-oxo-C12-HSL, respectively.

2. Material and methods

2.1. Molecular docking protocol validation

Protein Data Bank (PDB) was searched for LuxS from *B. subtilis* and LasI from *P. aeruginosa*. For LuxS from *B. subtilis*, a total of seven crystallographic protein structures and five ligands were retrieved for LuxS: 1J98 (resolution = 1.20 Å) and 1IE0 (resolution = 1.60 Å) as X-ray structures of LuxS; 2FQT (resolution = 1.79 Å) and 2FQO (resolution = 1.87 Å) which contained a X-ray structure of LuxS in complex with (2S)-2-amino-4-[(2R,3S)-2,3-dihydroxy-3-*N*-hydroxycarbamoyl-propylmercapto]butyric acid (H1D) and (2S)-2-amino-4-[(2R,3R)-2,3-dihydroxy-3-*N*-hydroxycarbamoyl-propylmercapto]butyric acid (HYI) – competitive inhibitors, respectively; 1JQW (resolution = 2.30 Å) as X-ray structure of LuxS/HCS complex; 1JVI (resolution = 2.20 Å) as LuxS/RHC complex; and, 1YCL (resolution = 1.80 Å) as LuxS complex with a catalytic 2-ketone intermediate (KRI). LuxS is a homodimeric metalloenzyme with two identical active sites, formed at the dimer interface by amino acid residues from both subunits. Each active site contains a zinc ion coordinated by the conservative residues His54, His58, and Cys126. RHC (substrate of catalytic reaction) binds in a deep pocket with the ribose moiety adjacent to the zinc ion (Ruzheinikov et al., 2001). As a starting point, 1JQW and 1JVI structures were selected to define the binding site. For 3-oxo-C12-HSL synthase, LasI from *P. aeruginosa*, a single X-ray crystallographic structure without ligands was retrieved – 1RO5 (resolution = 2.30 Å). The binding site of LasI is defined around amino acid residues such as Met79, Phe105, Thr142, and Thr144 (Gould et al., 2004). All crystallographic protein structures were prepared for docking, involving the removal of water and ligand molecules, the addition of hydrogen atoms, setting up bond orders and formal charges, and the definition of amino acid protonation states. The molecular docking/virtual screening protocol for LasR from *P. aeruginosa* was based on Magalhães at al. (2022). The selected PDB structure was 2UV0 (resolution = 1.80 Å), which contained an X-ray structure of LasR in complex with 3-oxo-C12-HSL.

For the optimization of molecular docking protocol, different docking software/scoring functions were adjusted: AutoDock VINA (Trott & Olson, 2010), GOLD (ChemPLP, GoldScore, ChemScore, and ASP) (Verdonk et al., 2003), and LeDock (Zhang & Zhao, 2016). Parameters adjusted with VINA included the box size and position, number of generated binding modes, and exhaustiveness. In GOLD, the parameters optimized were the radius of the binding site used in the exploration of the ligand-target conformational space, and the search efficiency (auto-scale). The radius was chosen to guarantee an overall volume consistent with the box size previously used with VINA. Finally, the binding site in LeDock was adjusted as referred for VINA. The box used as binding site of LuxS was centred on: x = 15.81, y = 36.83, and z = 83.48, and with dimensions: width = 19, height = 17, and depth = 18. Additionally, the box used as the binding site of LasR was centered on: x = 10.94, y = 4.39, and z = 19.98, with a radius of 5.66. For the LasI structure, the binding site was defined around the S-adenosyl-L-methionine (SAM) site: x = 48.61, y = -15.7, and z = -11.25, with a radius of 10.

Re-docking aimed to assess the quality of the molecular docking software/scoring function protocol in reproducing the known experimental binding pose of the crystallographic ligands in their specific target. For that, minimum Root Mean Square Deviation (RMSD, Å) calculations between docked and real pose for each specific target protein structure were performed using DockRMSD (Bell & Zhang, 2019). Cross-docking allowed to assess the ability of each structure to correctly accommodate ligands from other structures and measure its general usefulness. The average binding energy score from each molecular docking software/scoring function for all the ligands was calculated for each target protein. Note that score values from GOLD are dimensionless, and the higher score indicated a better binding affinity. VINA and LeDock calculate the binding energy in kcal/mol, and the more negative values suggested a better binding affinity.

2.2. Virtual screening protocol validation

Virtual screening protocol was validated by the ability to discriminate between real ligands (actives) and non-ligands (decoys). The ChEMBL database (https://www.ebi.ac.uk/chembl) was searched for active compounds against LuxS, reporting 16 distinct molecules. Decoys are compounds randomly generated with similar 1D physicochemical properties to actives, but distinct 2D topology. The Directory of Useful Decoys Enhanced (DUD-E, https://dude.docking.org/) retrieved a set of 50 decoys for each active compound. For 16 actives for LuxS, 800 decoys were generated, which corresponded to 788 distinct decoys. The previously optimized molecular docking protocols were applied to the active/decoys database. For LasI, 14 molecules were reported as active

compounds and 700 distinct decoys were generated.

The performance of different scoring functions in discriminating between actives/decoys can be evaluated by the calculation of the area under (AU) Receiver Operator Characteristic (ROC) curve. ROC curve is the plot of the true positive rate (TPR = TP/P) *versus* the false positive rate (FPR = FP/N), where TP is the number of true positives, FP is the number of false positives, P and N are the total number of positives (actives) and negatives (decoys), respectively. The higher the AU-ROC values, the better the discrimination between TP and FP. A random ranking corresponds to the equality line TPR = FPR, and AU-ROC of 0.5 (50%). The best scoring function should rank ligands early on a large score list. The enrichment factor at 1% (EF1%) and 20% (EF20%) measured the number of active ligands recovered at 1% and 20% of the active/decoys database, respectively, over the expected number of recovered active compounds using random scores. A high EF value in the first 1% means that the scoring function is better at discerning true active compounds early on (Miller et al., 2012). Ranked lists of active/decoys based on binding energy scores obtained with VINA, GOLD, and LeDock were used to determine AU-ROC, EF1% and EF20% (Empereur-Mot et al., 2016). At the end of this stage, an optimized virtual screening protocol was selected using the best performing molecular docking software/scoring function and crystallographic protein structures.

2.3. Virtual screening of a phytochemical database

The phytochemical database was developed by combining several online libraries: Analyticon (3608 compounds – https://ac-discovery.com/), Molport (1476 compounds – https://www.molport.com/shop/index), and PhytoHub (1674 compounds – https://phytohub.eu/). After the removal of duplicates, the phytochemical database comprised about 6133 compounds (only from plant sources). The database was limited by selecting compounds with specific properties associated with other drug-like compounds (3479 compounds) – *Lipinskís Rule of Five*: (a) the number of hydrogen bond donors ≤ 5; (b) the number of hydrogen bond acceptors ≤ 10; (c) molecular weight < 500 Da; (d) partition coefficient (logP) < 5 (Benet et al., 2016). The previously optimized virtual screening protocol was used to rank and evaluate the binding energy scores of phytochemicals to LuxS, LasI, and LasR. This approach allowed the selection of the most promising phytochemicals with potential anti-QS activity against LuxS/AI-2 and LasI/LasR QS systems for further experimental validation.

2.4. Bacterial strains and growth conditions

For *in vitro* assays, *B. subtilis* (Ehrenberg) Cohn (ATCC 6051) and *P. aeruginosa* PA14 wild-type were selected as representative strains for LuxS/AI-2 and LasI/LasR QS systems. The biosensor *P. aeruginosa* PA14-*R*3 reacts to 3-oxo-C12-HSL that is produced by *P. aeruginosa* PA14 wild-type and emits luminescence (Borges et al., 2017; Massai et al., 2011). *Vibrio harveyi* BB170 (ATCC BAA-1117) was selected as a reporter strain that produces bioluminescence in response to AI-2 from *B. subtilis*. *B. subtilis* and *P. aeruginosa* were grown in Luria-Bertani (LB, Sigma-Aldrich, USA) broth at 30 °C and 37 °C, respectively, with agitation (160 rpm). *V. harveyi* BB170 was cultivated in autoinducer bioassay broth (AB – 0.2% (*w/v*) DifcoTM casamino acids, vitamin assay (Thermofisher, USA), 50 mM magnesium sulfate heptahydrate (VWR, Belgium), 0.3 M sodium chloride (VWR, Belgium), 1 mM L-arginine (AlfaAesar, Germany), 1% (*v/v*) glycerol (VWR, Belgium), and 10 mM potassium phosphate buffer, at pH 7) at 30 °C, under 160 rpm of agitation.

2.5. Phytochemicals

Curcumin, 95% (total curcuminoid content), from *Turmeric rhizome* (Alfa Aesar, Germany), pioglitazone hydrochloride, 98% (Alfa Aesar, China), and 10-undecenoic acid, 99% (Alfa Aesar, Germany) were selected based on the *in silico* analysis. Phytochemical solutions were freshly prepared in 100% DMSO and the final concentration of DMSO used was 6% (*v/v*).

2.6. LuxS/AI-2 QS system

The inhibition of LuxS/AI-2 QS system of *B. subtilis* in the presence of the selected phytochemicals (through *in silico* analysis) was quantified using the reporter strain *V. harveyi* BB170, according to previous studies (Bassler et al., 1997; Taga & Xavier, 2011) with some modifications, as described in the following subsections.

2.6.1. Collection of cell-free fluid

B. subtilis was cultured aerobically in LB broth for 14 h at 30 °C with agitation (160 rpm). Afterwards, 5 mL of overnight culture was added to 95 mL of sterile LB (absorbance at 610 nm, $Abs_{610\ nm} = 0.1$, which corresponds to 4×10^6 CFU/mL) with a phytochemical solution at selected concentrations [curcumin at 1.25, 2.5, and 5 μg/mL; pioglitazone hydrochloride at 12.5, 25, and 50 μg/mL; and 10-undecenoic acid at 12.5, 25, and 50 μg/mL – values equal and lower than the minimum inhibitory concentrations (supplementary file)] and grown at 30 °C with agitation. Control samples were performed with DMSO. (Z-)-4-bromo-5-(bromomethylene)-2(5H)-furanone (Furanone C-30, Sigma-Aldrich, Switzerland) at 1 μM (6% (*v/v*) DMSO) was used as a positive control. Furanone C-30 was previously demonstrated to be a good inhibitor of LuxS, reducing the accumulation of AI-2 (Kuehl et al., 2009; Zang et al., 2009). The bacterial growth was monitored by the measure of Abs_{610nm} (spectrophotometer V-1200, VWR, China). A maximum cell density reduction of 20% in terms of absorbance was considered to minimize the unspecific effects of impaired growth on the QS response (Borges et al., 2017; Schultz et al., 2020). After 4.5 h of incubation, the suspension was centrifuged (2000*g*, 5 min) and 1 mL aliquots of the cell-free supernatant was collected and filtered [using a cellulose acetate syringe filter with a pore size of 0.22 μm (Whatman, VWR, Portugal)]. Cell-free culture fluid samples were frozen at −20 °C until the quantification of AI-2. The incubation time was previously optimized to obtain the maximum AI-2 accumulation, corresponding to the mid-exponential growth phase. Three independent experiments were performed for each condition tested.

2.6.2. Quantification of AI-2

V. harveyi BB170 from glycerol cryopreserved stock was inoculated into 5 mL of AB broth and incubated for 16 h at 30 °C, with 160 rpm of agitation (until $Abs_{600\ nm} = 1$). The brightness of culture was confirmed in a dark room. Afterwards, 2 μL of overnight culture was added to 20 mL of sterile AB broth. For quantification of AI-2, at least six wells of black 96-well flat opaque bottomed polystyrene (PS) microtiter plates (Thermo Fisher Scientific, Denmark) were filled with 20 μL of cell-free culture fluid (of each condition) and 180 μL of *V. harveyi* BB170 culture. For each measurement, the following control samples were performed: negative control – 20 μL of 6% (*v/v*) DMSO:LB and 180 μL of AB broth; and medium control – 20 μL of 6% (*v/v*) DMSO:LB or phytochemical:LB and 180 μL of *V. harveyi* BB170 culture. The luminescence (light counts per second, LCPS) was measured every 30 min for 9 h using a microtiter plate reader (Synergy HT, Biotek Instruments, USA) at 30 °C. Relevant parameters for bioluminescence assessment were: measurement interval time, 1 s; emission, hole; and gain, 200. For each condition, AI-2 accumulation was quantified as the difference between the bioluminescence of the sample and the related medium control, when the minimum value of luminescence was reached. Compared to the control culture (without phytochemicals), the cut-off value for QS inhibition was 15%.

2.7. LasI/LasR QS system

The ability of the selected phytochemicals to interfere with the LasI/

LasR QS system of *P. aeruginosa* was assessed by a high-throughput QS inhibition screening system based on the co-cultivation of *P. aeruginosa* PA14 wild-type and *P. aeruginosa* PA14-*R*3 (Massai et al., 2011). Briefly, *P. aeruginosa* PA14 wild-type and *P. aeruginosa* PA14-*R*3 from glycerol cryopreserved stock were grown overnight at 37 °C on LB agar plates – LB with 1.5% (*w/v*) agar (VWR Chemical, Belgium). Afterwards, bacteria were scraped from the plate surfaces, suspended in sterile LB broth, and adjusted to $Abs_{600\ nm}$ of 0.045 (7.2×10^7 CFU/mL) and 0.015 (3.0×10^7 CFU/mL) for *P. aeruginosa* PA14-*R*3 and *P. aeruginosa* PA14 wild-type, respectively. Black 96-well flat, opaque bottomed PS microtiter plates were filled with 180 μL of the co-culture and 20 μL of phytochemical solution at the concentrations selected (curcumin at 12.5, 50, and 200 μg/mL; pioglitazone hydrochloride at 62.5, 250, and 1000 μg/mL; and 10-undecenoic acid at 62.5, 250, and 1000 μg/mL). Furanone C-30 at 10 μM (6% (*v/v*) DMSO) was used as a positive control against LasI/LasR QS system by blocking the LasR receptor *i.e.* direct completion with 3-oxo-C12-HSL (Markus et al., 2021). Control samples were performed using cell suspension with DMSO (without phytochemical) and sterile LB broth with phytochemical solution (without cell suspension). After incubation at 37 °C for 4 h with agitation (160 rpm), the bioluminescence (LCPS) was measured using a microtiter plate reader (FLUOstar Omega, BMG Labtech, Germany). Relevant parameters for bioluminescence measurement were: measurement interval time, 1 s; emission, lens; and gain, 3600. The number of CFU per well (CFU/well) was determined in plate count agar (PCA, VWR, Belgium) after appropriate serial dilution in sterile saline solution and incubation at 37 °C for 24 h. CFU counts were performed since the applied phytochemical concentrations caused a high increase in absorbance compared to the control samples, due to phytochemical precipitation. In this study, a maximum cell density reduction of 30% of CFU/well was considered to minimize the unspecific effects of impaired growth on the QS response. This assumption was established by analyzing CFU/well range in assays without adding potential growth inhibitors. The luminescence values were normalized, dividing the LCPS by CFU/well. Three independent assays were performed with at least six replicates.

The reduction of luminescence of co-culture with phytochemical compared to control without phytochemical (at least 15%) suggested an active phytochemical against LasI/LasR QS system. These phytochemicals were selected for the following assays to evaluate the QS target – LasI (production of 3-oxo-C12-HSL) and/or LasR (detection/recognition of 3-oxo-C12-HSL).

2.7.1. Effects on LasI – Production of 3-oxo-12-HSL

The influence of the selected phytochemicals on the production of 3-oxo-C12-HSL was evaluated according to the method proposed by Massai et al. (2011). *P. aeruginosa* PA14 wild-type from a glycerol cryopreserved stock was grown overnight at 37 °C on LBA. Then, bacteria were scraped from the plate surfaces and diluted in LB broth to $Abs_{600\ nm}$ of 0.050 (5.50×10^7 CFU/mL). Nine mL of cell suspension were added to 50 mL centrifuge tubes along with 1 mL of phytochemical solution at selected concentrations (curcumin at 12.5, 50, and 200 μg/mL; pioglitazone hydrochloride at 62.5, 250, and 1000 μg/mL; and 10-undecenoic acid at 15.625, 62.5, and 250 μg/mL). Furanone C-30 at 10 μM (6% (*v/v*) DMSO) was used as a positive control. After 12 h of incubation at 37 °C with agitation (160 rpm), cell suspensions were centrifuged (Eppendorf® centrifuge 5810R, Germany) for 20 min at 3772*g* and the supernatants were collected and filtered (0.22 μm pore size syringe filter). The supernatants were stored at −20 °C until used. At least three independent experiments were performed for each condition tested. Black 96-well flat, opaque bottomed PS microtiter plates were filled with 20 μL of supernatant and 180 μL of *P. aeruginosa* PA14-*R*3 cell suspension, prepared as previously described for PA14 but diluted in LB broth to $Abs_{600\ nm} = 0.045$. After growth for 4 h (160 rpm, 37 °C), the luminescence was measured using a microtiter reader, and the number of CFU/well was determined by CFU counting onto PCA plates (maximum of 30% of CFU/well reduction). The luminescence values were normalized, dividing LCPS by CFU/well. At least six wells were analyzed for each condition.

A calibration curve was generated with 3-oxo-C12-HSL (Sigma-Aldrich, India) at known concentrations and used to calculate the concentration of 3-oxo-C12-HSL in each sample. For that, *P. aeruginosa* PA14-*R*3 was grown in the presence of increasing concentrations of synthetic 3-oxo-C12-HSL (0.305 nM to 15 μM, 6% (*v/v*) DMSO). Both linear and logarithmic regression lines were drawn from the normalized LCPS values (supplementary file, Figure S1). The calibration curves were performed in triplicate with six repeats, for each concentration. Then, for each condition, 3-oxo-C12-HSL was quantified and normalized to the cell culturability (Log CFU/well).

2.7.2. Effects on LasR – Detection of 3-oxo-12-HSL

The influence of the selected phytochemicals on the detection of 3-oxo-C12-HSL was evaluated according to a similar protocol as in section 2.5.1. For that, *P. aeruginosa* PA14-*R*3 from a glycerol cryopreserved stock was grown overnight at 37 °C on LBA. Then, bacteria were scraped from the plate surfaces and diluted in LB broth to $Abs_{600\ nm} = 0.045$ (7.2×10^7 CFU/mL). Black 96-well flat, opaque bottomed PS microtiter plates were filled with 180 μL of cell suspension, 10 μL of 50 μM synthetic 3-oxo-C12-HSL, and 10 μL of phytochemical solution at the selected concentrations (curcumin at 12.5, 50, and 200 μg/mL; pioglitazone hydrochloride at 62.5, 250, and 1000 μg/mL; and 10-undecenoic acid at 15.625, 62.5, and 250 μg/mL). The LCPS and CFU/well values were determined after growth for 4 h (maximum of 30% of CFU/well reduction). The luminescence values were normalized by dividing LCPS by CFU/well. The tests were performed in triplicate, with six repeats.

2.8. Statistical analysis

Computational data from the molecular docking and virtual screening studies were analyzed using the average and standard deviation (SD) tools of Microsoft Excel. The mean and SD within samples were calculated for all conditions. Experimental data were analyzed using Dunnett's multiple comparisons test and Tukey's multiple comparisons test (one-way ANOVA multiple comparations) from the statistical program GraphPad Prism 6.0 for Windows (GraphPad software, La Jolla California, USA). Statistical differences were established for a probability level of 95% ($P < 0.05$).

3. Results

3.1. Molecular docking and virtual screening protocol validation

A curated strategy for the optimization of molecular docking and virtual screening protocols for both LuxS/AI-2 QS system from *B. subtilis* and LasI/LasR QS system from *P. aeruginosa* was adopted. For that, re-docking of the ligands, for which there was crystallographic ligand-target structure available, was performed using different molecular docking software/scoring functions. Assuming a cut-off value for the RMSD between docked and crystallographic ligand poses around 2 Å, all molecular docking software/scoring functions showed good performance in re-docking ligands, except for 1JQW/HCS (Table 1). Additionally, ChemPLP was the molecular docking software/scoring function with the worst overall RMSD. In this specific case, checking the poses by visual inspection revealed an inverted ligand pose. The chemical interaction of the metal ion (zinc) and the terminal carboxy group of both ligands resulted in low binding score for the inverted pose. LeDock was the best performing molecular docking software/scoring function with an average RMSD of 0.9 Å.

From the cross-docking of five ligands using different molecular docking software/scoring functions, the average binding energy score was recovered for each target protein structure (Table 2). The LuxS protein structure 1IE0 showed the worst performance for all ligands using all molecular docking software/scoring functions. The best results,

Table 1
Re-docking RMSD (Å) values between docked and crystallographic ligand pose for each specific target protein structure for all molecular docking software/scoring functions used.

Receptor	Ligand	Molecular docking software/Scoring functions					
		VINA	ChemPLP	GoldScore	ChemScore	ASP	LeDock
1JVI	RHC	0.94	6.69	7.15	1.14	1.04	0.84
1YCL	KRI	1.68	7.56	1.02	1.02	0.92	0.68
1JQW	HCS	6.53	7.64	7.78	7.67	0.46	0.54
2FQT	H1D	1.98	6.76	2.07	2.02	2.69	1.72
2FQO	HYI	1.74	7.74	1.36	1.76	2.97	0.29
Average[a]		1.6 ± 0.4	7.2 ± 0.5	2.9 ± 2.5	1.5 ± 0.4	1.9 ± 0.9	0.9 ± 0.5

[1] Re-docking RMSD values for 1JQW/HCS were not included in the mean ± SD calculations.

Table 2
Average binding energy scores of ligands for each LuxS structure for all molecular docking software/scoring functions used. Values are the means ± SDs of binding energy scores of five tested ligands.

Receptor	Molecular docking software/Scoring functions					
	VINA	ChemPLP	GoldScore	ChemScore	ASP	LeDock
1IE0	−0.08 ± 0.08	27 ± 3	35 ± 5	5 ± 3	4 ± 3	−3.8 ± 0.4
1J98	−7.0 ± 0.2	80 ± 3	74 ± 2	24 ± 5	31 ± 0.7	−7.9 ± 0.2
1JVI	−7.4 ± 0.3	78 ± 3	78 ± 3	29 ± 3	33 ± 0.8	−8.2 ± 0.3
1YCL	−7.3 ± 0.2	85 ± 4	81 ± 2	36 ± 1	34 ± 1	−7 ± 2
1JKW	−6.5 ± 0.4	72 ± 3	77 ± 3	27 ± 2	31 ± 0.6	−7.5 ± 0.2
2FQT	−7.0 ± 0.3	85 ± 4	79 ± 4	29 ± 2	31 ± 0.7	−7.8 ± 2
2FQO	−7.1 ± 0.2	81 ± 4	75 ± 2	30 ± 3	32 ± 0.3	−8.0 ± 0.2
Average[a]	−6.6 ± 1.0	75 ± 11	72 ± 10	28 ± 5	29 ± 6	−7.1 ± 1.5

[1] Binding energy scores of ligands for 1IE0 were not included in mean ± SD calculations.

with high binding energy scores, were obtained using ChemPLP, followed by GoldScore, LeDock, and VINA. Results of re-docking and cross-docking suggested 1YCL and 2FQT as the best performing LuxS structures for the analysis conducted.

Virtual screening of a specifically built active/decoys database was performed for 1YCL and 2FQT, and different statistical tools were used to compare the performance of molecular docking software/scoring functions in giving a ranked list of active/decoys – Table 3. VINA, ASP, and LeDock failed to identify positive actives in 1% and 20% of the active/decoys database. ChemPLP was evaluated as the best molecular docking software/scoring function for virtual screening of the phytochemicals database (high EF1% and AU-ROC = 94–96). Despite the relatively high RMSD values (Table 1), this was considered non-limiting since ChemPLP had the best performance in discriminating confirmed actives from decoys. For all the other virtual screening simulations, ChemPLP also performed as the best molecular docking software/scoring function: for LasI, AU-ROC = 63.2, EF1% = 0.00, EF20% = 2.15 (6 recovered actives), EF (max) = 3.40; for LasR, AU-ROC = 76.0, EF1% = 10.2 (9 recovered actives), EF20% = 2.33 (42 recovered actives), EF (max) = 12.8.

3.2. Virtual screening of a phytochemical database

The previously optimized virtual screening protocol was used to rank and evaluate the binding energy scores of phytochemicals in LuxS, LasI, and LasR to attain potential inhibitors against both LuxS/AI-2 and LasI/LasR QS systems. The final phytochemical selection was based on a high binding score against QS receptors (LuxS and LasR). Furthermore, the binding score was also inspected against LasI. Other selection criteria were high availability and low cost. Thus, for LuxS, among the top 10 phytochemicals for both protein structures (1YCL and 2FQT), 10-undecenoic acid was identified as a potential QS inhibitor (binding score of 102). This phytochemical was also among the top 100 of LasI and LasR (binding score of 82). From the binding scores of LasR, among the top 50

Table 3
Performance of molecular docking software/scoring functions in the discrimination between active and decoys for 1YCL and 2FQT structures.

		Molecular docking software/Scoring functions					
		VINA	ChemPLP	GOLDScore	ChemScore	ASP	LeDock
1YCL	EF1%	0.00	31.3	12.6	12.6	0.00	0.00
	Recovered Actives (1%)	0	5	3	2	0	0
	Recovered Decoys (1%)	9	4	6	7	9	9
	EF20%	0.94	4.70	4.40	3.45	0.31	2.20
	Recovered Actives (20%)	3	15	14	11	1	7
	Recovered Decoys (20%)	158	146	147	150	160	154
	EF (Max)	2.20	31.3	18.3	18.5	1.80	2.90
	AU-ROC	63.7	94.0	87.9	85.4	62.0	68.5
2FQT	EF1%	0.00	18.8	6.27	6.27	0.00	0.00
	Recovered Actives (1%)	0	4	2	1	0	0
	Recovered Decoys (1%)	9	5	7	8	9	9
	EF20%	0.31	4.70	4.39	2.51	0.31	1.26
	Recovered Actives (20%)	1	15	14	8	1	4
	Recovered Decoys (20%)	160	146	147	153	160	157
	EF (max)	1.94	26.4	50.1	8.35	1.52	1.65
	AU-ROC	59.8	96.2	87.8	81.0	53.8	61.7

phytochemicals, curcumin and pioglitazone hydrochloride were identified (binding scores of 93 and 94, respectively). These two phytochemicals were present among the top 500 of LasI and LuxS (binding scores ranging between 64–67 and 72–77, respectively). These natural compounds comply with all of the requirements appointed above. The binding scores of phytochemicals were compared with that of natural QS ligands of each target protein (*i.e.* RHC, SAM, and 3-oxo-C12-HSL – substrates of catalytic reactions on LuxS, LasI, and LasR, respectively) – Table 4. All phytochemicals showed binding scores close to natural QS ligands, demonstrating favourable chemical interaction with QS targets. Binding scores of phytochemicals higher than that of natural QS ligands could reveal more favourable competition by the active binding site. Thus, curcumin and pioglitazone hydrochloride had a slightly higher probability to interact with LasR than natural QS ligands. Additionally, 10-undecenoic acid could strongly interact with LuxS and LasI. Predicted interactions suggested that the selected phytochemicals could be promising binders able to inhibit AIs production and/or its detection. Thus, *in vitro* analyses were performed to confirm if lead phytochemicals have effectively potential QS inhibition against LuxS of *B. subtilis* and LasI/LasR of *P. aeruginosa*.

3.3. Effects of phytochemicals on QS systems

Any phytochemical able to interfere with QS system without cell density reduction was considered a good QS inhibitor. Based on AI-2 measurement, relative AI-2 reduction (%) in the presence of phytochemicals was determined in comparison to the control sample (*B. subtilis* culture without phytochemicals) – Fig. 1. Pioglitazone hydrochloride did not cause a reduction of AI-2 accumulation in cultures (<15%). Curcumin and 10-undecenoic acid caused a significant AI-2 reduction at the concentrations tested. The best phytochemicals against LuxS/AI-2 QS system were curcumin (33–77%) followed by 10-undecenoic acid (36–64%). It is worth mentioning that both phytochemicals caused higher QS inhibition than furanone, a known QS inhibitor. The QS inhibitory activity of curcumin was dose-dependent, as increasing concentration from 2.5 to 5 μg/mL significantly increased AI-2 reduction ($P < 0.05$).

From high-throughput QS inhibition screening results against *P. aeruginosa* (Fig. 2), curcumin and 10-undecenoic acid were also found to be potential QS inhibitors. Their performance was significantly different, while curcumin caused lower activity (28–37%) than furanone (66%), 10-undecenoic acid triggered the highest reduction (79–88%) of LasI/LasR QS system. The phytochemical concentrations tested did not affect cell density, except 1000 μg/mL of 10-undecenoic acid. Therefore, for this phytochemical a lower concentration was applied for the subsequent analysis – 15.625 μg/mL.

Additional assays were conducted to determine the specific target of curcumin and 10-undecenoic acid on LasI/LasR QS system. Fig. 3 shows the QS inhibitory activity targeting LasI (3-oxo-C12-HSL production) and LasR (3-oxo-C12-HSL detection), respectively. Compared to the control sample (without phytochemicals), 10-undecenoic acid (15.625–250 μg/mL) promoted a 28–54% reduction of 3-oxo-C12-HSL production, while curcumin only caused a significant reduction for the highest concentration tested (200 μg/mL, 21%) ($P < 0.05$). Additionally,

Table 4
Binding scores using ChemPLP for the interaction of natural QS ligands (RHC, SAM, and 3-oxo-C12-HSL – substrates of catalytic reactions on LuxS, LasI, and LasR, respectively) and the phytochemicals against LuxS of *B. subtilis* and LasI/LasR of *P. aeruginosa*.

	LuxS	LasI	LasR
Natural ligands	RHC	SAM	3-oxo-C12-HSL
	86.1	68.0	90.6
Curcumin	72.4	64.5	92.8
Pioglitazone hydrochloride	77.1	66.9	94.3
10-Undecenoic acid	102	82.4	82.0

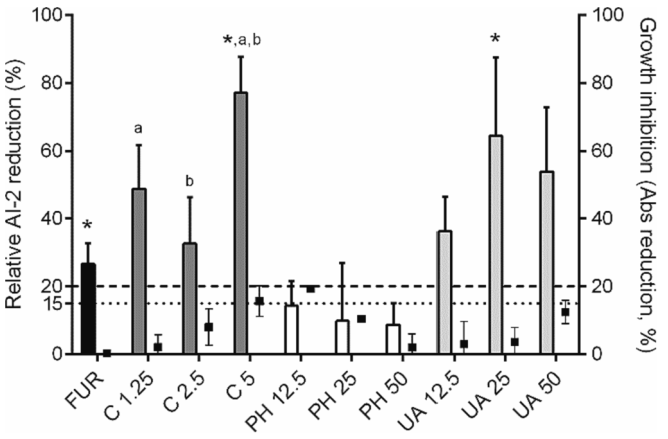

Fig. 1. Relative AI-2 reduction for *B. subtilis* cultures in the presence of curcumin (C), pioglitazone hydrochloride (PH), and 10-undecenoic acid (UA) at different concentrations (in μg/mL) (left-y axis; bars). Effects on cell density as $Abs_{610\ nm}$ reduction (right-y axis; dots). Positive control corresponded to relative AI-2 reduction of culture in presence of furanone (FUR). Dashed lines correspond to cut-off values for the maximum growth inhibition (20% of $Abs_{610\ nm}$) and minimum QS inhibition (15%). * – Relative AI-2 reduction in the presence of phytochemicals was statistically different from furanone (Dunnett's multiple comparisons test, $P < 0.05$). [a] and [b] – AI-2 accumulation was statistically different between different concentrations of each phytochemical (Tukey's multiple comparisons test, $P < 0.05$). Values are the means ± SDs of three independent experiments.

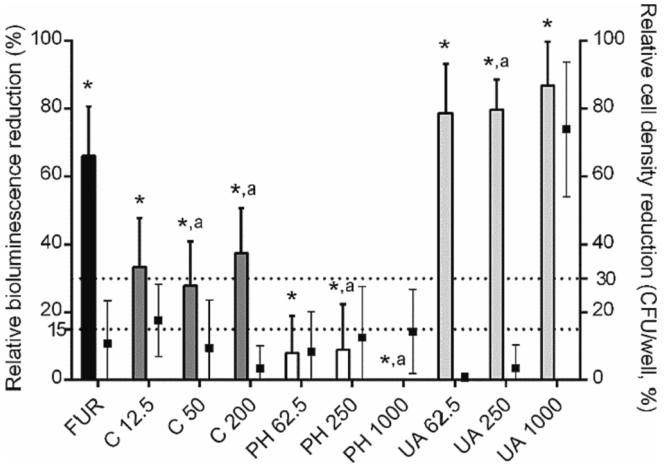

Fig. 2. Relative bioluminescence reduction (%) for the co-culture of *P. aeruginosa* in the presence of curcumin (C), pioglitazone hydrochloride (PH), and 10-undecenoic acid (UA) at different concentrations (in μg/mL) (left-y axis; bars). Effects on cell density as CFU/well reduction (right-y axis; dots). Positive control corresponded to relative bioluminescence reduction in the presence of furanone (FUR). Dashed lines correspond to cut-off values for the maximum growth inhibition (30% of CFU/well) and minimum QS inhibition (15%). * – Relative bioluminescence reduction in the presence of phytochemicals was statistically different from furanone (Dunnett's multiple comparisons test, $P < 0.05$). [a] – Relative bioluminescence reduction was statistically different between concentrations for each phytochemical (Tukey's multiple comparisons test, $P < 0.05$). Values are the means ± SDs of three independent experiments.

10-undecenoic acid caused higher effects on 3-oxo-C12-HSL detection than curcumin (10–26% and 0–7%, respectively). The effects on LasI and LasR were found to be dose-dependent, increasing phytochemical concentration significantly decreased 3-oxo-C12-HSL production and decreased relative bioluminescence (low ability to recognize external 3-oxo-C12-HSL), respectively ($P < 0.05$).

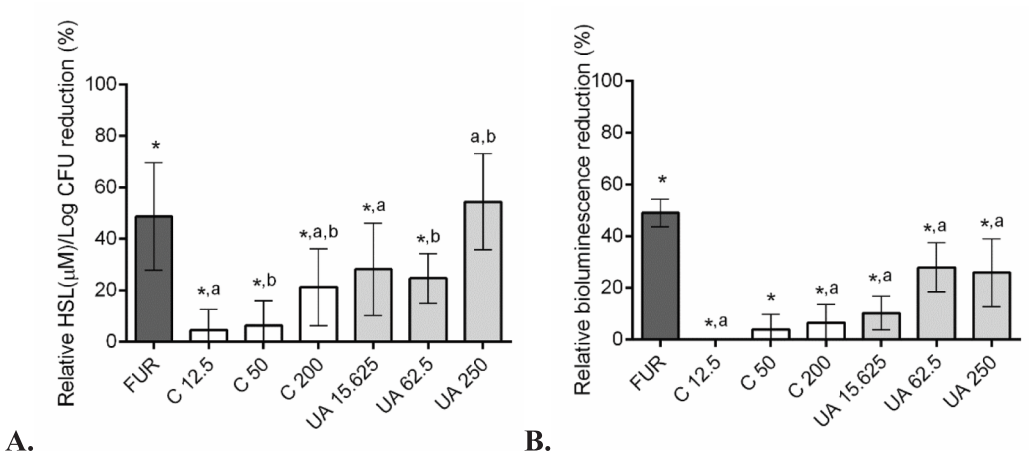

Fig. 3. Effects of curcumin (C) and 10-undecenoic acid (UA) at different concentrations (in μg/mL) – on production (LasI, **A**) and detection (LasR, **B**) of 3-oxo-C12-HSL. Positive control corresponded to cultures in the presence of furanone (FUR). The relative HSL/Log CFU and relative bioluminescence reduction were determined relative to the control sample (without phytochemicals). * – Relative reduction in the presence of phytochemicals was statistically different from furanone (Dunnett's multiple comparisons test, $P < 0.05$). [a] and [b] – relative reduction was statistically different between different concentrations of each phytochemical (Tukey's multiple comparisons test, $P < 0.05$).

4. Discussion

Molecular docking and virtual screening have been applied to predict the interaction of molecules against specific targets (Puertas-Martin et al., 2020). Its application allowed the selection of small datasets from a large chemical database to be experimentally tested. Although the incorrect recognition of false positives or false negatives, this approach is faster and showed higher accuracy than if it was done by traditional laboratory methods (Puertas-Martin et al., 2020). This type of analysis recognizes the potential of new molecules that otherwise would remain unexploited. Recently, several authors developed and applied molecular docking/virtual screening to identify potential QS inhibitors, but without experimental validation. For example, QS inhibitors against LasR from *P. aeruginosa* (Dalal et al., 2022; Sadiq et al., 2020) and CviR from *Chromobacterium violaceum* (Martins et al., 2021). Other authors have successfully used this methodology to identify QS inhibitors against specific QS targets of one bacterial strain (Ding et al., 2019; Mellini et al., 2019; Shukla et al., 2021; Zhong et al., 2020) and to corroborate QS inhibition by chemical interactions with the specific QS targets. For example, LasR/RhlR and LasR/FabI from *P. aeruginosa* (Bose et al., 2020; Mansuri et al., 2020), LuxS from *Streptococcus suis* (Li et al., 2021), Agr from *Staphylococcus aureus* (Oliveira et al., 2021), and PcoR from *P. fluorescens* (Yu et al., 2022). The present study focused on the optimization and validation of a virtual screening protocol to pick phytochemicals with potential anti-QS activity against both LuxS/AI-2 QS from *B. subtilis* and LasI/LasR QS of *P. aeruginosa*, followed by *in vitro* validation. The QS systems of *B. subtilis* and *P. aeruginosa* have been intensively studied and reviewed by several authors (Bareia et al., 2018; Duplantier et al., 2021; Zhang et al., 2020). *B. subtilis* is a model of Gram-positive bacterium for biofilm formation, due to its high ability to form structurally diverse biofilms under different environmental conditions (Duanis-Assaf et al., 2015; Morikawa, 2006). Previous work demonstrated that biofilm formation by *B. subtilis* was induced by AI-2 accumulation, which is mediated by LuxS activity (Lombardia et al., 2006). Additionally, other authors verified that the presence of lactose prompts biofilm formation through the activation of LuxS pathway, increasing AI-2 production (Duanis-Assaf et al., 2015). In another way, *P. aeruginosa* is a model Gram-negative bacterium used for the development of anti-virulence drugs (Duplantier et al., 2021). This bacterium can quickly develop antimicrobial resistance, being on the top of the WHO priority list for the development of new antibiotics (Tacconelli et al., 2018). *P. aeruginosa* cause acute and chronic infections with a high mortality rate and antibiotic failure, due to the expression of virulence factors mainly regulated by QS (Brindhadevi et al., 2020; Duplantier et al., 2021). Thus, affecting these QS systems could effectively control biofilm formation and bacterial virulence, processes that are related to LuxS/AI-2 QS and LasI/LasR QS system (Duanis-Assaf et al., 2015; Whitehead et al., 2001).

The optimized virtual screening protocol allowed the identification of curcumin, pioglitazone hydrochloride, and 10-undecenoic acid as the most promising QS inhibitors of LuxS of *B. subtilis* and LasI/LasR of *P. aeruginosa*. The optimized virtual screening protocol was successful as only pioglitazone hydrochloride was identified as a false positive – absence of anti-QS activity – due to inherent docking errors. Pioglitazone hydrochloride is the hydrochloride salt of an orally active thiazolidinedione with antidiabetic properties and potential antineoplastic activity (Masadeh et al., 2011). Its antimicrobial activity was demonstrated against Gram-positive (*Streptococcus pneumoniae*) and Gram-negative (*E. coli* and *K. pneumoniae*) bacteria (Masadeh et al., 2011). These authors also verified an increase in antibiotic susceptibility after previous exposure to a sub-inhibitory concentration of that molecule. Recently, Croppi et al. (2020) concluded that the antimicrobial activity of pioglitazone hydrochloride is related to a high level of reactive oxygen species generation via suppression of H_2S-producing enzymes. In this study, although its antimicrobial activity and promising results of *in silico* screening, *in vitro* assays did not suggest relevant effects on both QS systems tested.

Curcumin is a major constituent of turmeric (*Curcuma longa*) and is known for its antimicrobial, antitumour, antiallergic, anti-inflammatory, and antioxidant activity (Kunnumakkara et al., 2017; Moghadamtousi et al., 2014). It is generally recognized as safe (GRAS) by the Food and Drug Administration (FDA) (FDA, 2017). However, curcumin has limited applications due to its low solubility and bioavailability. The potential of curcumin to reduce *P. aeruginosa* virulence and biofilm formation by inhibiting QS system has been demonstrated (Abdulrahman et al., 2020; Sethupathy et al., 2016). Other authors identified curcumin as a QS inhibitor of LasR by *in silico* analysis and subsequent suppression of biofilm formation and other virulence factors (Shukla et al., 2021). In this study, curcumin was identified as a QS inhibitor against not only the LasI/LasR QS but also against the LuxS/AI-2 QS system. In terms of LasI/LasR QS system, curcumin (at 200 μg/mL) caused a 21% reduction of 3-oxo-C12-HSL production by *P. aeruginosa* PA14. This behaviour was also verified by Rudrappa & Bais (2008) that achieved a 25% reduction of 3-oxo-C12-HSL production by *P. aeruginosa* PAO1 exposed to a sub-inhibitory concentration of curcumin (at 1 μg/mL). Inhibition of biofilm formation and diverse virulence factors, like pyocyanin biosynthesis and elastase/protease activity, were also observed (Rudrappa & Bais, 2008). The same authors reported a MIC value for curcumin of 30 μg/mL instead of the 200 μg/mL found in this study. These differences in concentrations could be related to the bacterial strains used and the purity/availability of curcumin. Additionally, it was verified that curcumin (at 1.25–5 μg/mL) caused a reduction of AI-2 accumulation in *B. subtilis*. Other authors found repression of gene expression related to LuxS/AI-2 QS system of

Streptococcus mutants when using curcumin at 184 μg/mL (Li et al., 2018).

10-undecenoic acid is a monounsaturated fatty acid derived from castor oil (from the beans of the castor plant, *Ricinus Communis*, of the *Euphorbiceae* family). It has antifungal, antiviral, and antibacterial activity (Shi et al., 2016; Van der Steen & Stevens, 2009). 10-undecenoic acid is considered by EPA Safer Chemical Ingredients List as safe for preservative and antioxidant purposes (preferred human and environmental health profiles) (EPA , 2020). Additionally, no hazard effect level for inhalation and dermal route and low hazard for eye route was identified for this molecule (ECHA, 2022). Both LuxS/AI-2 and LasI/LasR QS systems from *P. aeruginosa* and *B. subtilis*, respectively, were affected by the presence of 10-undecenoic acid. To the best of the authors' knowledge, this study was the first demonstrating QS inhibition by this molecule, that caused similar or higher effects than furanone and curcumin. Previous research identified several long-chain fatty acids (linoleic acid, stearic acid, oleic acid, and palmitic acid) as LuxS/AI-2 QS inhibitors using the reporter strain *V. harveyi* BB170 (Widmer et al., 2007). Other authors demonstrated the anti-QS activity of agaric acid (another fatty acid) against *Salmonella* by inhibiting biofilm formation through the reduction of flagellar motility (a QS-regulated mechanism) (Lories et al., 2020). Distinct antimicrobial effects from fatty acids can be obtained due to different chemical properties, such as carbon saturation, chain length, molecular configuration, hydrogenation, and hydroxylation (Kumar et al. 2020). The validation of another fatty acid (10-undecenoic acid) as anti-QS compound can support the potential of fatty acids as anti-biofilm agents.

For a general understanding of the chemical interactions between validated phytochemicals with anti-QS activity (curcumin and 10-undecenoic acid) and specific QS targets, molecular dynamic simulations should be performed to explain their mode of action (Magalhães et al., 2022). Furthermore, since the down-regulation of QS during antimicrobial treatment resulted in the mitigation of pathogens and microbial virulence (Li et al., 2022), the combination of curcumin and/or 10-undecenoic acid with other current antimicrobial agents (antibiotics or biocides) could help to recover or potentiate their antimicrobial activity.

5. Conclusion

An optimized virtual screening protocol permitted a reliable identification of new potential QS inhibitors from a phytochemical drug-like database against both LuxS/AI-2 QS of *B. subtilis* and LasI/LasR QS of *P. aeruginosa*. *In silico* analysis revealed curcumin, pioglitazone hydrochloride, and 10-undecenoic acid as potential QS inhibitors. *In vitro* assays corroborated the QS inhibitory activity for curcumin (1.25–200 μg/mL) and 10-undecenoic acid (12.5–250 μg/mL), however, pioglitazone hydrochloride had no *in vitro* effect (false positive). Therefore, QS inhibitory activity of curcumin and 10-undecenoic against *B. subtilis* and *P. aeruginosa* was reinforced by *in silico* and *in vitro* analysis. 10-undecenoic acid was the strongest QS inhibitor, promoting similar or even higher anti-QS effects than curcumin. The safety and low toxicity of these phytochemicals, as corroborated by the GRAS status of curcumin and the safety of 10-undecenoic acid for preservative and antioxidant purposes, highlight the potential for a secure application in translational research for biofilm control.

CRediT authorship contribution statement

Susana Fernandes: Conceptualization, Methodology, Validation, Formal analysis, Investigation, Writing – original draft, Funding acquisition. **Anabela Borges:** Investigation, Writing – review & editing. **Inês B. Gomes:** Investigation, Writing – review & editing. **Sérgio F. Sousa:** Conceptualization, Methodology, Resources, Writing – review & editing, Supervision. **Manuel Simões:** Conceptualization, Methodology, Resources, Writing – review & editing, Supervision, Project administration, Funding acquisition.

Declaration of Competing Interest

The authors declare that they have no known competing financial interests or personal relationships that could have appeared to influence the work reported in this paper.

Data availability

Data will be made available on request.

Acknowledgements

This work was financially supported by: LA/P/0045/2020 (ALiCE), UIDB/00511/2020 and UIDP/00511/2020 (LEPABE), funded by national funds through FCT/MCTES (PIDDAC); Projects POCI-01-0247-FEDER-072237, funded by FEDER funds through COMPETE2020—Programa Operacional Competitividade e Internacionalização (POCI) and by national funds (PIDDAC) through FCT/MCTES; national funds from Fundação para a Ciência e a Tecnologia (grant numbers: UIDP/04378/2020, UIDB/04378/2020, and 2020.01423.CEECIND/CP1596/CT0003); Project HealthyWaters (NORTE-01-0145-FEDER000069), supported by Norte Portugal Regional Operational Programme (NORTE 2020) under the PORTUGAL 2020 Partnership Agreement through the European Regional Development Fund (ERDF), and by the FCT PhD scholarship attributed to Susana Fernandes (FCT/SFRH/BD/147276/2019). Anabela Borges thanks the FCT for the financial support of her work contract through the Scientific Employment Stimulus–Individual Call–[CEECIND/00823/2021]. Sérgio F. Sousa thanks FCT for grant 2020.01423.CEECIND.

Appendix A. Supplementary material

Supplementary data to this article can be found online at https://doi.org/10.1016/j.foodres.2023.112519.

References

Abdulrahman, H., Misba, L., Ahmad, S., & Khan, A. U. (2020). Curcumin induced photodynamic therapy mediated suppression of quorum sensing pathway of *Pseudomonas aeruginosa*: An approach to inhibit biofilm in vitro. *Photodiagnosis and Photodynamic Therapy, 30*, Article 101645.

Atkinson, S., & Williams, P. (2009). Quorum sensing and social networking in the microbial world. *Journal of the Royal Society, Interface, 6*(40), 959–978.

Bali, E. B., Turkmen, K. E., Erdonmez, D., & Saglam, N. (2019). Comparative study of inhibitory potential of dietary phytochemicals against quorum sensing activity of and biofilm formation by *Chromobacterium violaceum* 12472, and swimming and swarming behaviour of *Pseudomonas aeruginosa* PAO1. *Food Technology and Biotechnology, 57*(2), 212–221.

Bareia, T., Pollak, S., & Eldar, A. (2018). Self-sensing in *Bacillus subtilis* quorum-sensing systems. *Nature Microbiology, 3*(1), 83–89.

Bassler, B. L., Greenberg, E. P., & Stevens, A. M. (1997). Cross-species induction of luminescence in the quorum-sensing bacterium *Vibrio harveyi*. *Journal of Bacteriology, 179*(12), 4043–4045.

Bell, E. W., & Zhang, Y. (2019). DockRMSD: An open-source tool for atom mapping and RMSD calculation of symmetric molecules through graph isomorphism. *J Cheminform, 11*(1), 40.

Benet, L. Z., Hosey, C. M., Ursu, O., & Oprea, T. I. (2016). BDDCS, the Rule of 5 and drugability. *Advanced Drug Delivery Reviews, 101*, 89–98.

Borges, A., Sousa, P., Gaspar, A., Vilar, S., Borges, F., & Simões, M. (2017). Furvina inhibits the 3-oxo-C12-HSL-based quorum sensing system of *Pseudomonas aeruginosa* and QS-dependent phenotypes. *Biofouling, 33*(2), 156–168.

Bose, S. K., Chauhan, M., Dhingra, N., Chhibber, S., & Harjai, K. (2020). Terpinen-4-ol attenuates quorum sensing regulated virulence factors and biofilm formation in *Pseudomonas aeruginosa*. *Future Microbiology, 15*(2), 127–142.

Bottomley, M. J., Muraglia, E., Bazzo, R., & Carfi, A. (2007). Molecular insights into quorum sensing in the human pathogen *Pseudomonas aeruginosa* from the structure of the virulence regulator LasR bound to its autoinducer. *The Journal of Biological Chemistry, 282*(18), 13592–13600.

Bozzoli, F., Cattani, L., & Rainieri, S. (2020). Cross-helix corrugation: The optimal geometry for effective food thermal processing. *International Journal of Heat and Mass Transfer, 147*, Article 118874.

Brindhadevi, K., LewisOscar, F., Mylonakis, E., Shanmugam, S., Verma, T. N., & Pugazhendhi, A. (2020). Biofilm and quorum sensing mediated pathogenicity in *Pseudomonas aeruginosa*. *Process Biochemistry, 96*, 49–57.

Chakraborty, P., Dastidar, D. G., Paul, P., Dutta, S., Basu, D., Sharma, S. R., … Tribedi, P. (2020). Inhibition of biofilm formation of *Pseudomonas aeruginosa* by caffeine: A potential approach for sustainable management of biofilm. *Archives of Microbiology, 202*(3), 623–635.

Croppi, G., Zhou, Y., Yang, R., Bian, Y., Zhao, M., Hu, Y., … Wu, F. (2020). Discovery of an inhibitor for bacterial 3-mercaptopyruvate sulfurtransferase that synergistically controls bacterial survival. *Cell Chemical Biology, 27*(12), 1483–1499.

Dalal, A., Kushwaha, T., Choudhir, G., Inampudi, K. K., Karmakar, T., Hariprasad, P., & Gholap, S. L. (2022). Computational investigations on the potential role of hygrophorones as quorum sensing inhibitors against LasR protein of *Pseudomonas aeruginosa. J Biomol Struct Dyn, Jan 25*, 1-11.

Ding, T., Li, T., & Li, J. (2019). Discovery of quorum sensing inhibitors of *Pseudomonas fluorescens* P07 by using a receptor-based pharmacophore model and virtual screening. *LWT, 109*, 171–178.

Duanis-Assaf, D., Steinberg, D., Chai, Y., & Shemesh, M. (2015). The LuxS based quorum sensing governs lactose induced biofilm formation by *Bacillus subtilis*. *Frontiers in Microbiology, 6*, 1517.

Duplantier, M., Lohou, E., & Sonnet, P. (2021). Quorum sensing inhibitors to quench *P. aeruginosa* pathogenicity. *Pharmaceuticals (Basel), 14*(12), 1262.

ECHA. (2022). Undec-10-enoic acid - Toxicological summary. Retrieved from https://echa.europa.eu/pt/registration-dossier/-/registered-dossier/10078/7/1. Accessed July, 2022.

Empereur-Mot, C., Zagury, J. F., & Montes, M. (2016). Screening explorer - an interactive tool for the analysis of screening results. *Journal of Chemical Information and Modeling, 56*(12), 2281–2286.

EPA, U. (2020). Safer chemical ingredients list. Retrieved from https://www.epa.gov/saferchoice/safer-ingredients#searchList. Accessed May, 2021.

FDA, U. (2017). GRAS Notice 686, Curcumin from turmeric (*Curcuma longa* L.).

Fernandes, S., Gomes, I. B., Sousa, S. F., & Simões, M. (2022). Antimicrobial susceptibility of persister biofilm cells of *Bacillus cereus* and *Pseudomonas fluorescens*. *Microorganisms, 10*(1), 160.

Gould, T. A., Schweizer, H. P., & Churchill, M. E. (2004). Structure of the *Pseudomonas aeruginosa* acyl-homoserinelactone synthase LasI. *Molecular Microbiology, 53*(4), 1135–1146.

Hawver, L. A., Jung, S. A., & Ng, W. L. (2016). Specificity and complexity in bacterial quorum-sensing systems. *FEMS Microbiology Reviews, 40*(5), 738–752.

Hintz, T., Matthews, K. K., & Di, R. (2015). The use of plant antimicrobial compounds for food preservation. *Biomed Research International, 2015*, Article 246264.

Kim, H. S., Lee, S. H., Byun, Y., & Park, H. D. (2015). 6-Gingerol reduces *Pseudomonas aeruginosa* biofilm formation and virulence via quorum sensing inhibition. *Scientific Reports, 5*, 8656.

Kuehl, R., Al-Bataineh, S., Gordon, O., Luginbuehl, R., Otto, M., Textor, M., & Landmann, R. (2009). Furanone at subinhibitory concentrations enhances staphylococcal biofilm formation by luxS repression. *Antimicrobial Agents and Chemotherapy, 53*(10), 4159–4166.

Kumar, P., Lee, J. H., Beyenal, H., & Lee, J. (2020). Fatty acids as antibiofilm and antivirulence agents. *Trends in Microbiology, 28*(9), 753–768.

Kunnumakkara, A. B., Bordoloi, D., Padmavathi, G., Monisha, J., Roy, N. K., Prasad, S., & Aggarwal, B. B. (2017). Curcumin, the golden nutraceutical: Multitargeting for multiple chronic diseases. *British Journal of Pharmacology, 174*(11), 1325–1348.

Li, B., Li, X., Lin, H., & Zhou, Y. (2018). Curcumin as a promising antibacterial agent: effects on metabolism and biofilm formation in *S. mutans*. *Biomed Res Int, 2018*, 4508709.

Li, G., Tang, L., Zhang, X., & Dong, J. (2019). A review of factors affecting the efficiency of clean-in-place procedures in closed processing systems. *Energy, 178*, 57–71.

Li, J., Fan, Q., Jin, M., Mao, C., Zhang, H., Zhang, X., … Wang, Y. (2021). Paeoniflorin reduce luxS/AI-2 system-controlled biofilm formation and virulence in *Streptococcus suis*. *Virulence, 12*(1), 3062–3073.

Li, Y., Wang, H., Xu, C., Sun, S. H., Xiao, K., & Huang, X. (2022). Two strategies of stubborn biofouling strains surviving from NaClO membrane cleaning: EPS shielding and/or quorum sensing. *The Science of the Total Environment, 838*(Pt 3), Article 156421.

Lombardia, E., Rovetto, A. J., Arabolaza, A. L., & Grau, R. R. (2006). A LuxS-dependent cell-to-cell language regulates social behavior and development in *Bacillus subtilis*. *Journal of Bacteriology, 188*(12), 4442–4452.

Lories, B., Belpaire, T. E. R., Yssel, A., Ramon, H., & Steenackers, H. P. (2020). Agaric acid reduces *Salmonella* biofilm formation by inhibiting flagellar motility. *Biofilm, 2*, Article 100022.

Magalhães, R. P., Vieira, T. F., Melo, A., & Sousa, S. F. (2022). Identification of novel candidates for inhibition of LasR, a quorum-sensing receptor of multidrug resistant *Pseudomonas aeruginosa*, through a specialized multi-level *in silico* approach. *Molecular Systems Design & Engineering, 7*(5), 434–446.

Mansuri, A., Lokhande, K., Kore, S., Gaikwad, S., Nawani, N., Swamy, K. V., … Pawar, S. (2020). Antioxidant, anti-quorum sensing, biofilm inhibitory activities and chemical composition of Patchouli essential oil: *In vitro* and *in silico* approach. *Journal of Biomolecular Structure & Dynamics, Aug 24*, 1–12.

Markus, V., Golberg, K., Terali, K., Ozer, N., Kramarsky-Winter, E., Marks, R. S., & Kushmaro, A. (2021). Assessing the molecular targets and mode of action of furanone C-30 on *Pseudomonas aeruginosa* quorum sensing. *Molecules, 26*(6), 1620.

Martins, F. G., Melo, A., & Sousa, S. F. (2021). Identification of new potential inhibitors of quorum sensing through a specialized multi-Level computational approach. *Molecules, 26*(9), 2600.

Masadeh, M. M., Mhaidat, N. M., Al-Azzam, S. I., & Alzoubi, K. H. (2011). Investigation of the antibacterial activity of pioglitazone. *Drug Design, Development and Therapy, 5*, 421–425.

Massai, F., Imperi, F., Quattrucci, S., Zennaro, E., Visca, P., & Leoni, L. (2011). A multitask biosensor for micro-volumetric detection of N-3-oxo-dodecanoyl-homoserine lactone quorum sensing signal. *Biosensors & Bioelectronics, 26*(8), 3444–3449.

Mayer, C., Muras, A., Parga, A., Romero, M., Rumbo-Feal, S., Poza, M., … Otero, A. (2020). Quorum sensing as a target for controlling surface associated motility and biofilm formation in *Acinetobacter baumannii* ATCC(R) 17978(TM). *Frontiers in Microbiology, 11*, Article 565548.

Mellini, M., Di Muzio, E., D'Angelo, F., Baldelli, V., Ferrillo, S., Visca, P., … Rampioni, G. (2019). *In silico* selection and experimental validation of FDA-approved drugs as anti-quorum sensing agents. *Frontiers in Microbiology, 10*, 2355.

Miller, B. R., 3rd, McGee, T. D., Jr., Swails, J. M., Homeyer, N., Gohlke, H., & Roitberg, A. E. (2012). MMPBSA.py: An efficient program for end-state free energy calculations. *Journal of Chemical Theory and Computation, 8*(9), 3314–3321.

Moghadamtousi, S. Z., Kadir, H. A., Hassandarvish, P., Tajik, H., Abubakar, S., & Zandi, K. (2014). A review on antibacterial, antiviral, and antifungal activity of curcumin. *Biomed Research International, 2014*, Article 186864.

Morikawa, M. (2006). Beneficial biofilm formation by industrial bacteria *Bacillus subtilis* and related species. *Journal of Bioscience and Bioengineering, 101*(1), 1–8.

Ng, W. L., & Bassler, B. L. (2009). Bacterial quorum-sensing network architectures. *Annual Review of Genetics, 43*, 197–222.

Oliveira, D., Borges, A., Ruiz, R. M., Negrin, Z. R., Distinto, S., Borges, F., & Simões, M. (2021). 2-(2-Methyl-2-nitrovinyl)furan but not furvina interfere with *Staphylococcus aureus* Agr quorum-sensing system and potentiate the action of fusidic acid against biofilms. *International Journal of Molecular Sciences, 22*(2), 613.

Petit, J., Six, T., Moreau, A., Ronse, G., & Delaplace, G. (2013). β-lactoglobulin denaturation, aggregation, and fouling in a plate heat exchanger: Pilot-scale experiments and dimensional analysis. *Chemical Engineering Science, 101*, 432–450.

Puertas-Martin, S., Banegas-Luna, A. J., Paredes-Ramos, M., Redondo, J. L., Ortigosa, P. M., Brovarets, O. O., & Perez-Sanchez, H. (2020). Is high performance computing a requirement for novel drug discovery and how will this impact academic efforts? *Expert Opinion on Drug Discovery, 15*(9), 981–986.

Rudrappa, T., & Bais, H. P. (2008). Curcumin, a known phenolic from *Curcuma longa*, attenuates the virulence of *Pseudomonas aeruginosa* PAO1 in whole plant and animal pathogenicity models. *Journal of Agricultural and Food Chemistry, 56*, 1955–1962.

Ruzheinikov, S. N., Das, S. K., Sedelnikova, S. E., Hartley, A., Foster, S. J., Horsburgh, M. J., … Baker, P. J. (2001). The 1.2 A structure of a novel quorum-sensing protein, *Bacillus subtilis* LuxS. *Journal of Molecular Biology, 313*(1), 111–122.

Sadiq, S., Rana, N. F., Zahid, M. A., Zargaham, M. K., Tanweer, T., Batool, A., … Siddiqi, A. R. (2020). Virtual screening of FDA-approved drugs against LasR of *Pseudomonas aeruginosa* for antibiofilm potential. *Molecules, 25*(16), 3723.

Schauder, S., Shokat, K., Surette, M. G., & Bassler, B. L. (2001). The LuxS family of bacterial autoinducers: Biosynthesis of a novel quorum-sensing signal molecules. *Molecular Microbiology, 41*(2), 463–467.

Schultz, F., Anywar, G., Tang, H., Chassagne, F., Lyles, J. T., Garbe, L. A., & Quave, C. L. (2020). Targeting ESKAPE pathogens with anti-infective medicinal plants from the Greater Mpigi region in Uganda. *Scientific Reports, 10*(1), 11935.

Sethupathy, S., Prasath, K. G., Ananthi, S., Mahalingam, S., Balan, S. Y., & Pandian, S. K. (2016). Proteomic analysis reveals modulation of iron homeostasis and oxidative stress response in *Pseudomonas aeruginosa* PAO1 by curcumin inhibiting quorum sensing regulated virulence factors and biofilm production. *Journal of Proteomics, 145*, 112–126.

Shi, D., Zhao, Y., Yan, H., Fu, H., Shen, Y., Lu, G., … Liu, W. (2016). Antifungal effects of undecylenic acid on the biofilm formation of *Candida albicans*. *International Journal of Clinical Pharmacology and Therapeutics, 54*(5), 343–353.

Shukla, A., Shukla, G., Parmar, P., Patel, B., Goswami, D., & Saraf, M. (2021). Exemplifying the next generation of antibiotic susceptibility intensifiers of phytochemicals by LasR-mediated quorum sensing inhibition. *Scientific Reports, 11*(1), 22421.

Tacconelli, E., Carrara, E., Savoldi, A., Harbarth, S., Mendelson, M., Monnet, D. L., … Zorzet, A. (2018). Discovery, research, and development of new antibiotics: The WHO priority list of antibiotic-resistant bacteria and tuberculosis. *The Lancet Infectious Diseases, 18*(3), 318–327.

Taga, M. E., & Xavier, K. B. (2011). Methods for analysis of bacterial autoinducer-2 production. *Curr Protoc Microbiol, 23* (1), 1C.1.1-1C.1.15.

Trott, O., & Olson, A. J. (2010). AutoDock Vina: Improving the speed and accuracy of docking with a new scoring function, efficient optimization, and multithreading. *Journal of Computational Chemistry, 31*(2), 455–461.

Van der Steen, M., & Stevens, C. V. (2009). Undecylenic acid: a valuable and physiologically active renewable building block from castor oil. *ChemSusChem, 2*(8), 692–713.

Verdonk, M. L., Cole, J. C., Hartshorn, M. J., Murray, C. W., & Taylor, R. D. (2003). Improved protein-ligand docking using GOLD. *Proteins: Structure, Function, and Bioinformatics, 52*, 609–623.

Wei, L. N., Shi, C. Z., Luo, C. X., Hu, C. Y., & Meng, Y. H. (2020). Phloretin inhibits biofilm formation by affecting quorum sensing under different temperature. *Lwt, 131*, Article 109668.

Whitehead, N. A., Barnard, A. M., Slater, H., Simpson, N. J., & Salmond, G. P. (2001). Quorum-sensing in Gram-negative bacteria. *FEMS Microbiology Reviews, 25*(4), 365–404.

Widmer, K. W., Soni, K. A., Hume, M. E., Beier, R. C., Jesudhasan, P., & Pillai, S. D. (2007). Identification of poultry meat-derived fatty acids functioning as quorum sensing signal inhibitors to autoinducer-2 (AI-2). *Journal of Food Science, 72*(9), M363–M368.

Yu, H., Liu, Y., Yang, F., Xie, Y., Guo, Y., Cheng, Y., & Yao, W. (2022). The combination of hexanal and geraniol in sublethal concentrations synergistically inhibits quorum

sensing in *Pseudomonas fluorescens - in vitro* and *in silico* approaches. *Journal of Applied Microbiology, 133*(4), 2122–2136.

Zang, T., Lee, B. W., Cannon, L. M., Ritter, K. A., Dai, S., Ren, D., … Zhou, Z. S. (2009). A naturally occurring brominated furanone covalently modifies and inactivates LuxS. *Bioorganic & Medicinal Chemistry Letters, 19*(21), 6200–6204.

Zhang, B., Ku, X., Zhang, X., Zhang, Y., Chen, G., Chen, F., … He, Q. (2019). The AI-2/luxS quorum sensing system affects the growth characteristics, biofilm formation, and virulence of *Haemophilus parasuis*. *Frontiers in Cellular and Infection Microbiology, 9*, 62.

Zhang, L., Li, S., Liu, X., Wang, Z., Jiang, M., Wang, R., … Shen, X. (2020). Sensing of autoinducer-2 by functionally distinct receptors in prokaryotes. *Nature Communications, 11*(1), 5371.

Zhang, N., & Zhao, H. (2016). Enriching screening libraries with bioactive fragment space. *Bioorganic & Medicinal Chemistry Letters, 26*(15), 3594–3597.

Zhong, L., Ravichandran, V., Zhang, N., Wang, H., Bian, X., Zhang, Y., & Li, A. (2020). Attenuation of *Pseudomonas aeruginosa* quorum sensing by natural products: Virtual screening, evaluation and biomolecular interactions. *International Journal of Molecular Sciences, 21*(6), 2190.